Hexagonal Mn_2O_3 nanoplates as anode materials for lithium ion batteries

Hao Zheng[a], Qing Liu[b], Ting Wang[c], Jinsong Chen[d], Rongfei Zhao[e], Lin Li[f]

Key Laboratory of Functional Materials and Chemistry for Performance and Resource of Guizhou education department, Anshun University, Anshun 561000, China

[a]zhengaho1986@126.com, [b]496063041@qq.com, [c]390516278@qq.com, [d]85828082@qq.com, [e]44723318@qq.com, [f]lilin404003375@qq.com

Keywords: nanoplates, Mn_2O_3, anode material, Lithium ion batteries

Abstract: Hexagonal Mn_2O_3 nanoplates were synthesized by a hydrothermal method and then a annealing process. The Hexagonal Mn_2O_3 nanoplates prepared at hydrothermal temperature 200 ^oC exhibited the best electrochemical properties with a high reversible capability and cycling stability, It still retains a high capacity of 565 mAh g^{-1}, even after 100 cycles, as anode materials for lithium-ion batteries. The good electrochemical performance for the porous Mn_2O_3 microspheres can be attributed to its high surface area and mesoporous structure.

Introduction

Recently, a variety of metal oxides has been investigated as potential electrode materials for LIBs. Among the numerous candidates as LIB anodes, three representative types of metal oxides stand out with distinct lithium storage mechanisms and characteristics, namely tin dioxide[1], titanium dioxide[2], and many transition metal oxides.

Manganese oxides, which include MnO, MnO_2, Mn_2O_3, and Mn_3O_4, have received great interest recently with the advantages of earth-abundance, nontoxicity, and cost effectiveness[3, 4]. Among them, Mn_2O_3 electrode materials for LIBs have a high theoretical capacity of 1018 $mAhg^{-1}$ and lower operating voltage (average discharge voltage at 0.5 V and charge voltage at 1.2 V). Much attention has been paid to improve the cycling performance of Mn_2O_3[5-7].

In this work, we report that the hexagonal Mn_2O_3 nanoplates were synthesized by a hydrothermal method and then a annealing process. The electrochemical performances of the as-prepared hexagonal Mn_2O_3 nanoplates as anode materials of LIBs were also investigated.

Experimental

Synthesis and characterization of the samples

All chemicals were of analytical grade and were used without further purification. In a typical experiment, 0.5mmol $MnAc_2{\cdot}4H_2O$ was first dissolved in 30 mL deionized water at room temperature under magnetic stirring. Then 2 mL of $N_2H_4{\cdot}4H_2O$ (85%) was added into the above solution. The mixture was poured into and sealed in a Teflon-lined stainless steel autoclave of 50 mL capacity. The autoclave was heated to and maintained at 160-200 ^oC for 12 h and then air-cooled to room temperature. The product was collected by filtration, washed with distilled water and ethanol, and then dried under vacuum at 60 ^oC for 10 min. The obtained powders were heated in air at 600 ^oC for 4 h (at a heating rate of about 4 ^oC/min) to synthesize Mn_2O_3 nanoplates (denoted as Mn_2O_3-160, Mn_2O_3-180, and Mn_2O_3-200, respectively).

The crystallinity and structure of the samples were characterized by X-ray diffraction (XRD),

using a Rigaku X-ray diffractometer with Cu Kα radiation (λ = 1.5406Å). Scan electron microscopy (SEM) images were carried out with a VEGA3 TESCAN electron microscopy.

The electrochemical characterization was performed using CR2032 coin-type test cells. The cell consisted of a cathode with the composition of 70 wt.% active materials, 20 wt.% carbon black, and 10 wt.% PVDF, a lithium metal anode separated by a Celguard 2400 microporous film. The electrolyte was 1 $molL^{-1}$ $LiPF_6$/ (EC) and (DEC) (1:1). The charge–discharge tests were galvanostatically performed over 0.01 to 3.0 V at different current densities.

Results and discussion

The XRD pattern of the final products is depicted in Figure 1d. All the diffraction peaks in the XRD pattern can be indexed to body-centered cubic Mn_2O_3, according to the standard XRD data file (JCPDS file no. 78-0390). No peaks of impurities can be detected from the XRD pattern.

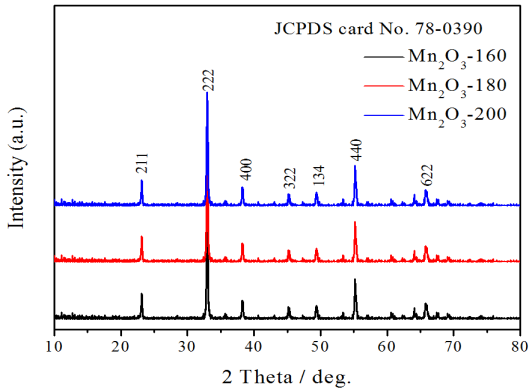

Fig. 1. XRD patterns of the Mn_2O_3 samples.

The surface morphological features of the samples were investigated by SEM in Fig.2. The products display a nanoplates structure without aggregation while still maintaining the original plate-like morphology. It is well known that the particle size, particle size distribution and morphologies of the samples will directly influence the electrochemical performance of the electrode materials. Considering their nanoplates structures favoring the diffusion of Li^+ ions and electrode−electrolyte contacts during the electrochemical reaction, the Mn_2O_3 nanoplates are expected to improve the electrochemical performance.

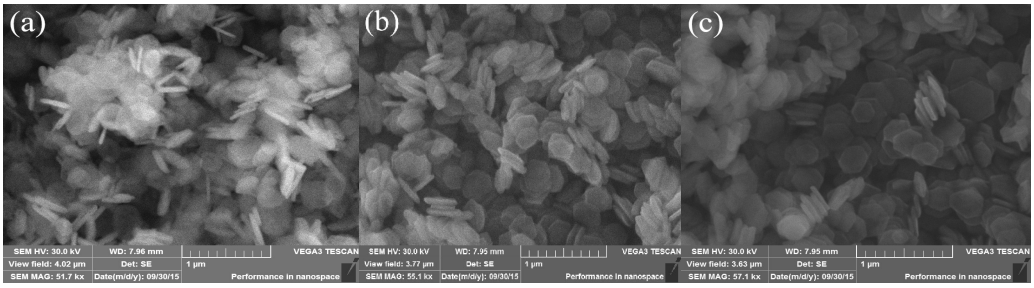

Fig. 2. SEM images of (a) Mn_2O_3-160, (b) Mn_2O_3-180, and (c)Mn_2O_3-200.

The electrochemical performances of Mn_2O_3 were measured via coin cell testing. Fig. 3 illustrates the discharge–charge profiles of the Mn_2O_3 nanoplates as anode materials for rechargeable lithium batteries at a current density of 100 mA g^{-1} at room temperature in a potential window between 0.01 and 3.0 V (versus Li^+/Li). From these, a large irreversible capacity at the first cycle is observed. The specific capacity of the Mn_2O_3-160 and Mn_2O_3-180 showed an obvious decrease with cycling, from 1047 and 1140 mAh g^{-1} for the first cycle to 597 and 598 mAh g^{-1} for the 100^{th} cycle, whereas Mn_2O_3-200 exhibits the best performance for Li^+ insertion, the Mn_2O_3-200 delivers a larger initial capacity of 1281 mAh/g and shows a high reversible capacity of 1147 mAh

g^{-1} for the second cycle, which is much higher than what was reported for those samples. which is higher than the theoretical value (1018 mAh g^{-1}). The excess capacities could be associated with the decomposition of the electrolyte at low voltages generating a solid electrolyte interphase (SEI) layer and the further lithium storage by interfacial charging at the metal/Li_2O interface. It still retains a high capacity of 620 mAh g^{-1} after 100 cycles. It is obvious that the Mn_2O_3-200 electrode shows much improved cycling performance with higher specific capacities at the same cycle with the same current density, as compared with the other samples, which may be attributed its bigger porous structure.

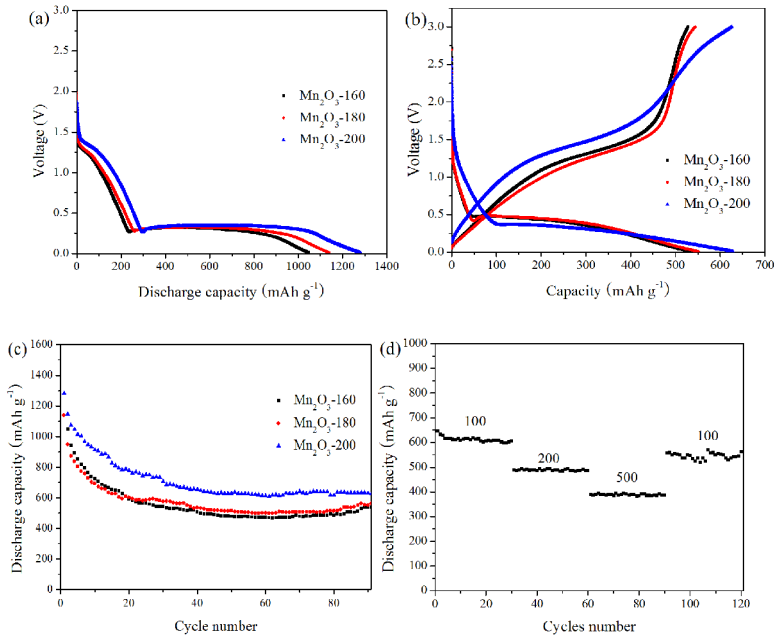

Fig. 3. (a) the first, (b) 100th discharge/charge curves and (c) cycling performance of the Mn_2O_3-160, Mn_2O_3-180, and Mn_2O_3-200; (d) cycling performance of the Mn_2O_3-200 electrode at various current densities.

To better understand the electrochemical behavior of the Mn_2O_3-200 nanoplates, we also investigated its rate performance as shown in Fig.3d. The cell shows good rate capability with average discharge capacity of 676, 489, and 389 mAh g^{-1} when the current density increased stepwise to 100, 200, and 500 mA g^{-1}, respectively. Upon altering the current density back to 100 mA g^{-1}, an average discharge capacity as high as 556 mAh/g could be recovered. These results demonstrate that the nanoplates structure Mn_2O_3 has great potential as high-rate anode material in lithium-ion batteries.

Conclusions

In summary, Mn_2O_3 nanoplates have been synthesized by a facile method. The Mn_2O_3-200 nanoplates exhibited a high reversible capacity of 1147 mAh g^{-1}, it still retains a high capacity of 620 mAh g^{-1}, even after 100 cycles at a current density of 100 mA g^{-1}. These results clearly demonstrate that the Mn_2O_3-200 nanoplates have better electrochemical performance with high specific capacity, long cycle life, and good rate capability, indicating that they are promising candidates for LIB anodes.

Acknowledgements

This work was financially supported by the joint science and technology funds of Guizhou Science

and Technology Department, Anshun city people’s government and Anshun university (grant No. LKA [2013]17, LH [2014] 7505).

References

[1] J.B. Goodenough and K.S. Park: J.Am. Chem. Soc. 135(2013), 1167–1176

[2] B. Kang and G. Ceder: Nature 458(2009), 190–193

[3] Y. Deng, L. Wan, Y. Xie and X. Qin: RSC Adv. 4 (2014), 23914–23935

[4] L. Chang, L.Q. Mai and X. Xu: RSC Adv. 3 (2013), 1947–1952

[5] X. Zhang, Y.T. Qian and Y.C. Zhu: Nanoscale 6 (2014), 1725–1731

[6]Y.H. Dai, H. Jiang and Y.J. Hu: RSC Adv. 3 (2013), 19778–19781

[7] J. F.Wang, G.Zhu and L.J. Deng: CrystEngComm 14 (2012), 8253–8260